

Structural models of metastable phases occurring during the crystallization process of saturated/unsaturated triacylglycerols

Oleksandr O. Mykhaylyk,^{a*} Kevin W. Smith,^b Christopher M. Martin^c and Anthony J. Ryan^a

^aDepartment of Chemistry, University of Sheffield, Sheffield, S3 7HF, UK, ^bUnilever Research and Development Colworth, Colworth House, Sharnbrook, MK44 1LQ, UK, and ^cCCLRC Daresbury Laboratory, Warrington, Cheshire, WA4 4AD, UK. Correspondence e-mail: o.mykhaylyk@shef.ac.uk

Isothermal crystallizations of saturated and mixed saturated/unsaturated triacylglycerols (TAGs) have been studied by simultaneous time-resolved small-angle and wide-angle X-ray scattering measurements (SAXS/WAXS). The projection of the electron density profile along the layer normal derived from the lamellar peaks of the α_2 -phase can be assembled from two types of molecular dimers initially formed in the liquid state. One dimer corresponds to a typical two-chain packing of TAGs and the other is formed by opposing molecules overlapping by their two-acyl-chain sides. This structure occurs only in triacylglycerols containing both saturated and unsaturated acyl chains. The structural organization of the α_2 -phase is analogous to smectic A interdigitated phases. In the particular case of 1,3-distearoyl-2-oleoyl-*sn*-glycerol, StOSt, the α_2 -phase can evolve into a mixture of two phases (α_1 and γ) with double and triple (2L and 3L) chain packing, respectively. A calculation of X-ray scattering patterns for simulated structures of randomly packed three-chain and two-chain layers of StOSt (2L + 3L) reproduced the three diffuse scattering peaks observed in the experimental SAXS patterns.

© 2007 International Union of Crystallography
Printed in Singapore – all rights reserved

1. Introduction

The common stable crystal structures of triacylglycerols (TAGs) are known to be the double- and triple-chain type of packing (2L and 3L, respectively) but there is growing evidence of another type of organization occurring at the very beginning of crystallization from the melt before the formation of the stable crystal structures. The transient metastable states are restricted to pure TAGs containing both saturated and unsaturated acyl chains (Kodali *et al.*, 1987; Takeuchi *et al.*, 2000; Ueno *et al.*, 1997) or mixtures thereof (Takeuchi *et al.*, 2002) including natural fats such as lard or cocoa butter (Loisel *et al.*, 1998; Rüner, 1970). Thus, to understand polymorphic transformations taking place in TAGs, especially in natural fats, the structures of various unstable phases have to be determined. Some attempts have already been made to interpret these structures with little or no success (Loisel *et al.*, 1998; Mykhaylyk & Hamley, 2004; Ueno *et al.*, 1997). The work presented herein extends the application of small-angle X-ray scattering (SAXS) methods to the structural analysis of stable phases in saturated/unsaturated 1,3-distearoyl-2-oleoyl-*sn*-glycerol (StOSt) (Mykhaylyk & Hamley, 2004) and is dedicated to modelling the structural organization of metastable phases appearing in saturated/unsaturated TAGs at the very beginning of their crystallization from the melt.

2. Materials and methods

Several triacylglycerols with sixteen and/or eighteen carbon atoms in the acyl chain have been investigated (Table 1) amongst which one

saturated TAG (tristearin, StStSt), solutions of saturated and unsaturated TAGs (StStSt and triolein, OOO, respectively) with mass ratio tristearin/triolein = 1:1 and 2:1, symmetric saturated/unsaturated triacylglycerols with *cis* conformation of the double bonds (StOSt, POP, StLnSt and PLnP) and non-symmetric saturated/unsaturated triacylglycerols (OOST and PPO) have been studied by simultaneous small-angle and wide-angle X-ray scattering (SAXS/WAXS) measurements. The TAGs have been investigated as received either from Sigma-Aldrich, Inc. (StStSt, OOO, StOSt and OOST) or from

Table 1

The evolution of the structural characteristics of the α_2 -phase (the period of layers, L , and the short d spacings) formed at the very beginning of isothermal crystallization of saturated/unsaturated TAGs during and after quenching from the melt.

TAG†	Initial stage		Final stage		Conditions of quenching
	L (Å)	d (Å)	L (Å)	d (Å)	
StOSt	54.3	4.09	51.5	4.20, 3.80	328 ⇒ 293 K
POP‡	52.0	n/a	n/a	n/a	323 ⇒ 253 K
StLnSt	54.4	4.11	52.5	4.13, 3.69	313 ⇒ 263 K
PLnP	51.9	4.10	49.9	4.17, 3.76	333 ⇒ 268 K
OOST	57.4	4.11	57.4	4.11	308 ⇒ 263 K
PPO	48.0	4.09	42.8	4.14, 3.72	328 ⇒ 253 K

† StOSt: 1,3-distearoyl-2-oleoyl-*sn*-glycerol; POP: 1,3-dipalmitoyl-2-oleoyl-*sn*-glycerol; StLnSt: 1,3-distearoyl-2-linolenoyl-*sn*-glycerol; PLnP: 1,3-dipalmitoyl-2-linolenoyl-*sn*-glycerol; OOST: 1,2-dioleoyl-3-stearoyl-*rac*-glycerol; PPO: 1,2-dipalmitoyl-3-oleoyl-*rac*-glycerol. ‡ A dominant α_1 -phase (2L packing) appears simultaneously, hiding diffraction peaks belonged to the α_2 -phase, thus the most of information is not available (n/a).

Unilever Research & Development, Colworth, UK (POP, StLnSt, PLnP and PPO) with purity of >99 wt.% each.

X-ray scattering patterns were recorded at the Synchrotron Radiation Source, Daresbury Laboratory, UK, on Station 6.2 with a small-angle camera length of 1.0 m and an X-ray wavelength $\lambda = 1.4 \text{ \AA}$. A one-dimensional quadrant detector and a one-dimensional curved linear detector RAPID 2 were used to record SAXS and WAXS data, respectively. Peak positions of a wet rat-tail collagen and a silicon standard (SRS 640c) were used to calibrate the q axis [$q = (4\pi/\lambda)\sin\theta$, where θ is half of the scattering angle] of the SAXS and WAXS patterns, respectively. The TAG samples were sealed in TA Instruments DSC aluminium pans. The pans were heated and cooled in a DSC instrument (Linkam, Tadworth, UK). Heating/cooling ramps were performed within the temperature interval 253–353 K at a rate of 30 K min^{-1} (Table 1). At the beginning of the thermal treatments each sample was kept for 2 min at a temperature >5 K above the melting point of the triacylglycerol and then quenched to the chosen temperature of isothermal crystallization. Time-resolved SAXS/WAXS patterns of TAGs were taken simultaneously at a time resolution between 2 and 30 s per frame during the thermal treatments.

The following equation was used to calculate projections of the electron density profile on the layer normal during the phase transformations of the TAGs.

$$S'(z) = \sum_{l=1}^{\infty} m(l)|F(l)| \cos\left(\frac{2\pi lz}{L}\right), \quad (1)$$

where z is a coordinate along the layer normal, l are the Miller indices of the lamellar peaks, $|F(l)|$ are the corresponding structural amplitudes obtained from SAXS patterns, L is the period of the lamellar

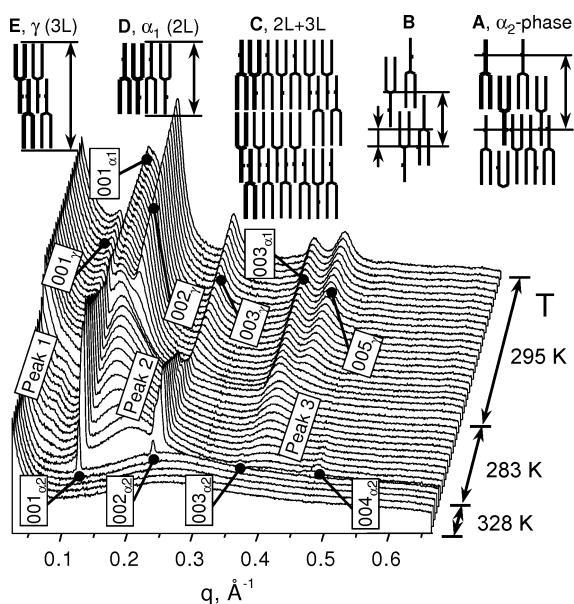


Figure 1 Time-resolved SAXS patterns (43 frames for 30 s each) of isothermal crystallization of StOst (intensity is plotted on a logarithmic scale) at 283 K quenched from the melt (328 K), followed by heating up to 295 K. Motifs of packing of the StOst molecules along the layer normal during the structural evolution of the α_2 -phase; C, mixed 2L and 3L packing; D, α_1 -phase (two-chain packing of the StOst); E, γ -phase (three-chain packing of the StOst). The arrows indicate the period of the layers. The boxed numbers indicate Miller indices of the lamellar peaks of the α_2 -, α_1 - and γ -phases of StOst. The three diffuse broad peaks corresponding to the mixed 2L + 3L packing of the StOst molecules (C) are numbered in the order of increasing q values.

structure and $m(l) = F(l)/|F(l)| = \pm 1$ are phase signs (Mykhaylyk & Hamley, 2004).

3. Scattering from lamellar structures comprising different types of layers with random stacking

In general, the relative intensity of an X-ray powder diffraction pattern can be expressed as

$$I(q) = KF(q)F^*(q)LPG, \quad (2)$$

where K represents all factors (including also both temperature and absorption factors) which are either constant or their deviations are negligible in the SAXS region and have been omitted in the further calculations; $LPG = (1 + \cos^2 2\theta)/(\sin^2 \theta \cos \theta)$ is a Lorentz–polarization–geometric factor and $F(q)$ are structural amplitudes. In the particular case of a one-dimensional lamellar structure with random alternation of different types of layers, the structural amplitude can be calculated as a sum of amplitudes of the layers $P_j(q)$ comprising the structure:

$$F(q) = (1/D) \sum_{j=1}^N P_j(q) \exp(-iqr_j), \quad (3)$$

where N is the number of layers along the calculated distance D , r_j is the position of the j th layer along the layer normal and $P_j(q) = \int_0^{L_j} S'_j(z) \exp(-iqz) dz$, where the integration is carried out over the thickness of the j th layer L_j and $S'_j(z)$ is a projection of the electron density profile on the layer normal of the j th layer. Thus, substituting equation (3) in equation (2), the equation describing the intensity from a lamellar structure formed from different types of layers with random stacking can be expressed as

$$I(q) = LPG \sum_{j=1}^N \sum_{k=1}^N \int_0^{L_j} S'_j(z) \exp[-iq(z + r_j)] dz \times \int_0^{L_k} S'_k(z) \exp[iq(z + r_k)] dz. \quad (4)$$

If both $S'_j(z)$ and the order of the layers in the lamellar structure are known, then the X-ray scattering pattern can be calculated using equation (4).

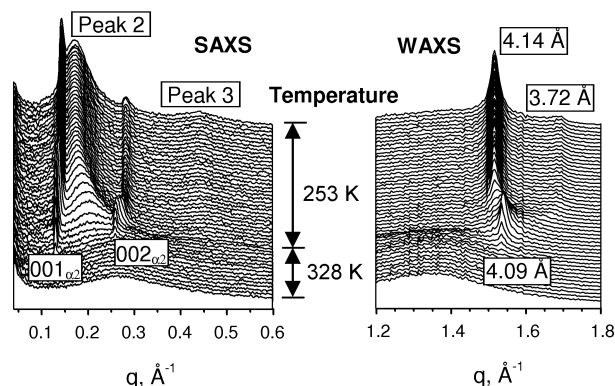


Figure 2 Time-resolved SAXS and WAXS patterns (49 frames for 2 s each) of isothermal crystallization of PPO (intensity is plotted on a logarithmic scale) at 253 K quenched from the melt (328 K). The boxed numbers indicate Miller indices of the lamellar peaks of the α_2 -phase of StOst. To be consistent with the StOst assignment (Fig. 1) the two diffuse broad peaks have been assigned as 'peak 2' and 'peak 3'.

4. Results and discussion

SAXS/WAXS time-resolved measurements of isothermal crystallization of either StStSt or solutions of StStSt/OOO have shown only formation of the α_1 -phase, corresponding to 2L packing of triacylglycerol molecules (Fig. 1D), whereas TAGs containing both saturated and unsaturated chains have demonstrated complex structural transformations at the very beginning of their crystallization. Initially the α_2 -phase appears which is characterized at the initial stage of formation by a set of sharp lamellar peaks in SAXS region and one relatively broad peak in WAXS corresponding to a d spacing of ~ 4.1 Å (Figs. 1 and 2, Table 1). The α_2 -phase has been identified previously in phase transformations of StOSt (Mykhaylyk & Hamley, 2004). These observations and others (Kodali *et al.*, 1987, 1990; Lavigne *et al.*, 1993; Lutton *et al.*, 1948) suggest that the formation of the α_2 -phase is totally dependent on the presence of both saturated and unsaturated acyl chains in TAG molecules.

Following a sequence of phase transformations taking place in StOSt during isothermal crystallization, a projection of the electron density profile on the layer normal of the α_2 -phase has been defined (Fig. 3a) and a corresponding packing of StOSt molecules with a 'twisted' structure of acyl chains has been suggested (Mykhaylyk & Hamley, 2004). Assuming this packing of StOSt molecules in the α_2 -phase, the mass density of this phase should be about 1.41 g cm $^{-3}$ (based on a lamellar period 54.3 Å and a hexagonal period of acyl chains in the lamellar $a_{\text{hex}} \sim 4.73$ Å), which is very large even in comparison with the most stable β -phases of TAGs [$\rho < 1.05$ g cm $^{-3}$ (Small, 1986)]. This unphysical estimate of density and the observation that the assigned structural amplitudes of the α_2 -phase had a poor agreement with the unique curve of structural amplitudes established for the α_1 -, γ - and β' -phases of StOSt (Mykhaylyk & Hamley, 2004) suggests that the real projection of the electron density profile on the layer normal of the α_2 -phase is different from that proposed previously.

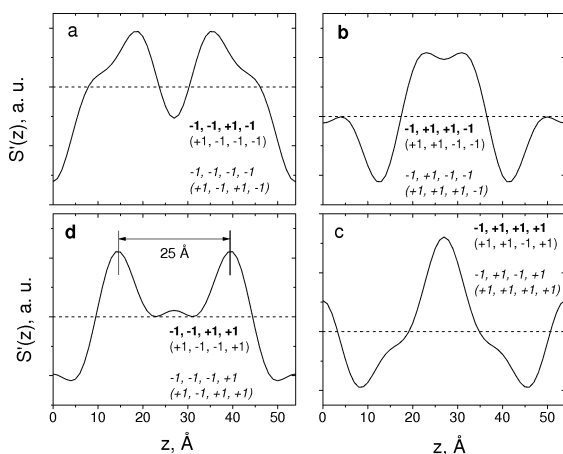


Figure 3
Four groups of projections of the electron density profile on the layer normal, $S'(z)$, which could be found from the intensities of the lamellar peaks of the α_2 -phase of StOSt (Mykhaylyk & Hamley, 2004) by a reciprocal Fourier transformation assuming that the lamellar structure is symmetric. The horizontal dashed lines indicate $S'(z) = 0$. The period of the α_2 -phase layer, $L\alpha_2$, is taken to be 54.3 Å. The number ones with negative and positive signs represent sixteen groups of four sign coefficients $[m(l), l = 1, \dots, 4]$ used for the calculation of the projections of the electron density profiles [equation (1)]. The coefficients in bold correspond to the projections of the electron density profiles presented in the graphs. The coefficients in italic produce similar shapes of the electron density profiles. The ones in brackets produce the same profiles of the electron densities but shifted by half of the period.

4.1. Defining a new structural model

Up to four diffraction lamellar peaks are usually observed for the α_2 -phase (see Figs. 1 and 2). Assuming that the structure has a symmetry which is typical in the structural organization of TAGs and lipids (de Jong *et al.*, 1991; Small, 1986), then 16 different variants ($= 2^4$) of phase signs of amplitudes in equation (1) and, therefore, 16 variants of $S'(z)$ could be obtained from the amplitudes. All these variants can be subdivided into four groups (see Fig. 3), one of which corresponds to the real structure. It has already been concluded that the first group (Fig. 3a) corresponding to a 'twisted' structure of acyl chains is unlikely to be real. Similarly the second and third groups of phase signs (Fig. 3b and c) also produce electron density profiles that are inconsistent with the molecular structure. One simple assumption is needed to correlate the molecular structure to the most appropriate set of phase signs. The TAG molecules are formed by attaching three unfolded acyl chains to a glycerol and the fact that the most intense peaks in the electron densities profiles of lipids (Torbet & Wilkins, 1976) and TAGs (Mykhaylyk & Hamley, 2004) correspond to the position of the most dense part of the molecules, that is the glycerol residue, leads to the conclusion that the fourth group of phase signs produces a projection of the electron density profile which requires serious attention (Fig. 3d). There are two pronounced density peaks separated from one another by a distance of ~ 25 Å, which corresponds to the projection of a glycerol residue of StOSt on the layer normal. This distance is consistent with the length of acyl chains forming an StOSt molecule (Fig. 4). The alternation of the higher density area and the lower density areas located between the glycerol residue peaks observed in the projection of the electron density profile (Fig. 3d) suggests that the structure could be created by two types of molecular dimers initially formed in a liquid state (Fig. 4). The formation of these dimers is driven by a packing incompatibility of the saturated and unsaturated acyl chains comprising the StOSt molecules (and other saturated/unsaturated TAGs). It is likely that only one type of dimer (Fig. 4, dimer 1) is formed in a liquid state of solely saturated or unsaturated TAGs (Small, 1986) leading directly

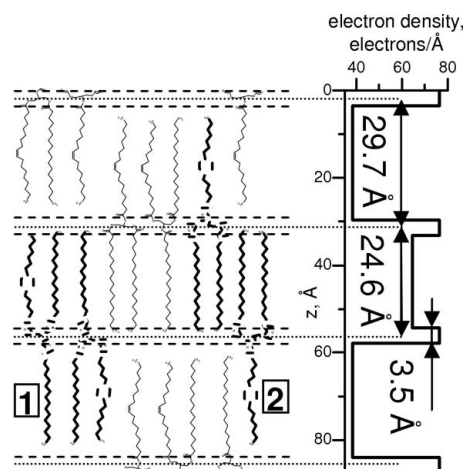


Figure 4
A model of the packing of the StOSt molecules in the layers of the α_2 -phase (left-hand side of the figure) and a fragment of the projection of the electron density distribution [presented by a strip model (Worthington, 1969)] of the molecules on the layer normal (right-hand side of the figure). The period of the layers in the shown fragment is 54.3 Å ($= 29.7 + 24.6$ Å). The largest value of the electron density corresponds to locations of the glycerol residues of the molecules in the layers (marked by the dashed lines). The molecules in bold represent models of packing of StOSt molecules in dimers (labelled by 1 and 2), which are likely to be formed in the liquid state before the formation of the α_2 -phase.

to the formation of the α_1 -phase (2L packing; Fig. 1D) at the very beginning of the crystallization of these TAGs. In TAGs with both saturated and unsaturated chains, however, random packing of two types of dimers, driven by a packing incompatibility of saturated and unsaturated acyl chains, should produce a lamellar structure with alternation of sublayers with a higher concentration of acyl chains (more populated sublayers) preferably populated by saturated chains and sublayers with slightly lower concentration of acyl chains (less populated sublayers) preferably populated by unsaturated chains (Fig. 4). A strip model of a projection of the electron density distribution on the layer normal (Worthington, 1969) of the random structure (Fig. 4, right-hand side) reproduces the main features observed in the electron density profile obtained from SAXS results (Fig. 3d).

4.2. Justification of the model

Using the molecular formula of StOSt ($C_{57}H_{108}O_6$) and the lamellar period of 54.3 Å, assuming hexagonal packing of acyl chains in the more populated sublayer ($a_{\text{hex}} = 4.73$ Å), an estimate of the mass density of the proposed structure can be obtained. If the structure of the α_2 -phase were formed by only one type of dimer (Fig. 4, dimer 1 or 2) then $\rho \simeq 0.97$ or 0.73 g cm⁻³, respectively. If the structure of the α_2 -phase is formed by a mixed composition of the dimers, as in the simulation of the electron density profile (Fig. 4) with a ratio of (dimer 1):(dimer 2) = 2:1, then $\rho \simeq 0.87$ g cm⁻³ and if the ratio is 4:1, then $\rho \simeq 0.91$ g cm⁻³, both of which are encompassed by the mass density of triacylglycerols in the liquid state (Small, 1986). These estimates clearly demonstrate that the mass density of the proposed structure of the α_2 -phase is below the mass densities known for stable triacylglycerol polymorphs (Small, 1986) and lies in the range between the mass density of a precursor liquid state and 0.97 g cm⁻³, corresponding to the densest packing of the StOSt dimers.

The proposed structure of the α_2 -phase has some empty space in the less populated sublayers and this provokes further phase transformations. Indeed, time-resolved SAXS/WAXS measurements of isothermal crystallization of PPO (Fig. 2) revealed that within 10 s of the beginning of the crystallization, when there are only lamellar peaks in the SAXS ($001\alpha_2$ and $002\alpha_2$) and one peak in the WAXS ($d = 4.09$ Å), two broad diffuse scattering peaks develop in the SAXS (peak 2 and peak 3) and the single hexagonal peak in the WAXS develops into two peaks ($d = 4.14$ and 3.72 Å), which could be interpreted as a reorganization of acyl chains into an orthorhombic subunit (Miller indices 110 and 200, respectively) typical of most olefins (Small, 1986). A similar observation has been made for most of the saturated/unsaturated TAGs studied in this work (Table 1) with the appearance of sharp lamellar peaks in the SAXS and a hexagonal peak in the WAXS at the very beginning of isothermal crystallization followed by the evolution of the positions of the lamellar peaks to larger q values, the transformation of the hexagonal peak into orthorhombic peaks and the formation of new diffuse scattering peaks. Apart from the appearance of a new diffuse scattering peak, OOST did not show either evolution of the positions of the lamellar peaks or the transformation from hexagonal to orthorhombic packing (Table 1).

4.3. Comparison with known structures

In general, the SAXS patterns of the α_2 -phase containing diffuse scattering peaks are similar to scattering effects observed in liquid crystal smectic A interdigitated phases identified in polar smectogenic compounds (Chan *et al.*, 1986). These phases usually exhibit one

or two quasi-Bragg peaks, corresponding to lamellar packing of the polar molecules, and a broad diffuse scattering peak generated by local defects formed by a mismatch in the packing of polar heads of the molecules within the lamellae. Following this analogy it can be suggested that after the initial formation of the α_2 -phase some TAG molecules undertake a further relocation driven by the packing incompatibility of saturated and unsaturated acyl chains that has its origin in the difference in their rotational isomeric states. As a result small regions with molecules shifted by a half of the length of the acyl chain can appear, generating two diffuse scattering peaks, one of which has a maximum corresponding to a d spacing equal to the sum of the length of one and half of the acyl chains and the length of a projection of the glycerol residue of the molecule on the layer normal and the second of which has a d spacing equal to the sum of the length of half of the acyl chains and the length of a projection of the glycerol part of the molecule on the layer normal. Taking the example of the lamellar packing of the α_2 -phase of StOSt, the shifting of the molecules is defined by the location of the carbon-carbon double bond in the oleoyl chain (Fig. 1B) generating diffuse scattering peaks at ~ 36 Å, peak 2, and ~ 14 Å, peak 3 (Fig. 1). This molecular reorganization may result in the release of more saturated chains, initially constrained by neighbouring unsaturated chains, enabling the formation of a periodic structure within the layer thereby leading to a tighter packing of these chains. This is observed as a transformation from hexagonal to orthorhombic in the WAXS which is contemporaneous with the appearance of the diffuse scattering peaks in the SAXS (Fig. 2).

The hypothesis of molecular reorganization is supported by the fact that OOST containing two unsaturated chains, where the stearoyl chains are unlikely to be released from neighbouring oleoyl chains during relocations of the OOST molecules in the α_2 -phase, does not show the hexagonal to orthorhombic transformation of the acyl chains (Table 1), in contrast to the rest of the TAGs studied herein, which have a single unsaturated chain. Moreover, the StLnSt and PLnP α_2 -phases demonstrated a very convincing transformation into orthorhombic packing with an intense diffraction peak, 200, which is likely to be a result of relocation of the TAG molecules facilitated by a strong incompatibility between saturated stearoyl (or palmitoyl) chains and polyunsaturated linolenoyl chains containing three carbon-carbon double bonds.

4.4. Interpretation of the transient features in the SAXS patterns

The majority of TAGs containing saturated and unsaturated chains (Table 1) have shown the formation of two diffuse scattering peaks (peaks 2 and 3 in Fig. 2) during transformation of the α_2 -phase during isothermal crystallization. These transformations have been shown to be strongly dependent on thermal treatments applied to the TAGs and comprehensive analysis of this phenomenon is beyond the scope of this work. It should be noted, however, that the α_2 -phase of PPO together with the diffuse scattering peaks observed at 253 K gradually evolve into a phase formed by 2L packing of TAGs (Fig. 2). The most interesting scattering effect in the SAXS patterns has been observed in structural transformations of the α_2 -phase of StOSt. At a certain point during the transformations a diffuse scattering peak at small q values corresponding to a d spacing of ~ 110 – 120 Å appears (peak 1, Fig. 1). This effect has been observed before in both StOSt (Mykhaylyk & Hamley, 2004) and cocoa butter (Loisel *et al.*, 1998), where StOSt is one of the main components, and it has been hypothesized that all three scattering peaks could be produced by a random distribution of two-chain and three-chain packed layers (or domains of these) stacked along the layer normal (Mykhaylyk &

Hamley, 2004). Indeed, if at some point of the transformation of the α_2 -phase the temperature is increased to a temperature 2 K below the melting point of the α_1 -phase of StOSt, the α_2 -phase transforms into a mixture of two phases: the 2L α_1 -phase and the 3L γ -phase of StOSt (Fig. 1). These observations suggest that StOSt molecules, after initially forming the metastable α_2 -phase from the melt, undergo further transformations creating domains of two-chain and three-chain packing of the molecules within the lamellar-like packing of the α_2 -phase and a slight increase in the temperature will supply enough energy to promote reorganization of the metastable structure into two types of phase-separated domains (α_1 -phase and γ -phase).

4.5. Quantitative simulations of SAXS for 2L + 3L packing in StOSt

The solution of the phase problem by reciprocal Fourier transformation, required to reproduce the projections of the electron density of both the 2L packing (α_1 -phase) and the 3L packing (γ -phase) on the layer normal from X-ray diffraction patterns, has been given recently (Mykhaylyk & Hamley, 2004). The distribution of the electron density for a layer of StOSt molecules with either 2L-chain type of packing or with 3L-chain type of packing [$S'(z)$] is available even without a knowledge of exact atomic positions within the layers. These data can be applied in simulations of X-ray scattering patterns of the proposed 2L + 3L structure using equation (4). To simulate the SAXS pattern we have assumed a random alternation of 2L and 3L packing of StOSt molecules along the layer normal. A Monte Carlo algorithm has been applied to generate the sequence of the 2L and 3L layers using a probability coefficient β and the following set of X-ray scattering patterns corresponding to a range of probability of 2L and 3L layers in the sequence of layers along the layer normal has been obtained (Fig. 5, inset). The pattern related to $\beta = 0.65$ (about half of

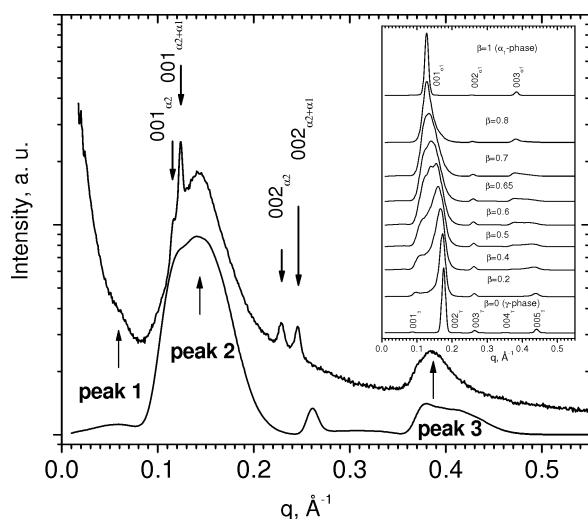


Figure 5

The experimental SAXS pattern of StOSt taken 6 min after the beginning of isothermal crystallization at 283 K after quenching from the melt (328 K) (frame 17, Fig. 1) compared to the simulated SAXS pattern of the lamellar structure of StOSt with random stacking of 2L and 3L packing with the ratio of the amount of the 2L and 3L layers being 3:2 ($\beta = 0.65$) corresponding to a structure containing one half of the molecules packed in the 2L layers and the other half in the 3L layers (the patterns are presented on a logarithmic scale). The inset shows a set of simulated SAXS patterns (on a linear scale) with different coefficients of probability (β) corresponding to the amount of the 2L layers in the structure ($\beta = 1$ and $\beta = 0$ correspond to structures with 2L and 3L packing only, respectively). The simulated patterns have been obtained as an average over an ensemble of 100 particles where each particle contains in total 30 2L and 3L layers randomly distributed along the layer normal. The Miller indices are assigned to the lamellar peaks.

StOSt molecules packed in the 2L layers and the other half in the 3L layers) reproduced most of the features observed in the experimental X-ray scattering of the α_2 -phase before the transformation into the α_1 - and γ -phases (Fig. 5). All three diffuse scattering peaks observed in the real pattern are generated by this structure with similar peak positions and relative intensities. It is suggested that the appearance of peak 1 after peak 2 and peak 3 in the time-resolved X-ray scattering of the isothermal crystallization of the α_2 -phase (Fig. 1) relates to an increase of the volume fraction of the StOSt molecules in the structure having a local packing of 5L chains (2L + 3L). The effect of the 2L + 3L chain packing is unique to StOSt amongst the TAGs studied herein. It is due to a close match of the length of the acyl chains comprising StOSt and its ability to form relatively stable 2L and 3L chain structures (Mykhaylyk & Hamley, 2004), hence peak 1 in the X-ray scattering patterns has been observed only for this triacylglycerol. A relatively sharp peak at $q = 0.26 \text{ \AA}^{-1}$ appears in the simulated SAXS patterns of the 2L + 3L structure (Fig. 5) and this is related to $002\alpha_1$ and 003γ and due to the fact that the projections of the electron densities on the layer normal are only available for the stable phases and not for the real 2L and 3L packing of the StOSt molecules formed during the transformations. A 2L and 3L period of packing of the molecules can be found, however, when this peak would disappear from the calculated X-ray scattering patterns using the curve of the structure factors corresponding to different types of packing of StOSt molecules (Mykhaylyk & Hamley, 2004). It should also be noted that in the SAXS pattern corresponding to the real structure, two sets of sharp peaks corresponding to two lamellar phases with periods 54.3 and 50.8 Å are also present (Fig. 5). The first set can originate from some residual α_2 -phase in the sample. Simulations of X-ray scattering, using a similar approach to that used for the 2L + 3L structure, found that the second set of peaks corresponding to the period 50.8 Å, which is in the region between the lamellar periods of the α_2 -phase and the α_1 -phase [49.1 Å (Mykhaylyk & Hamley, 2004)], may correspond to a structure formed by an alternation of layers of the α_2 -phase and the α_1 -phase growing within the α_2 -phase structure. This detail requires further studies to be undertaken to fully elucidate the nature of these lamellar peaks.

5. Conclusions

Time-resolved X-ray scattering has been used to study the isothermal crystallization of several TAGs. These represent the range of molecular compositions common in natural fats such as saturated TAGs, unsaturated TAGs, symmetric saturated/unsaturated triacylglycerols with *cis*-conformation of the double bonds and non-symmetric saturated/unsaturated triacylglycerols with *cis*-conformation of the double bonds. It has been found that TAGs comprising both saturated and unsaturated acyl chains show similar structural motifs at the very beginning of crystallization, identified as the α_2 -phase. The appearance of this phase is attributed to packing incompatibility of saturated and unsaturated chains present in the same molecule. The analysis of the projections of the electron density profile on the layer normal, obtained from intensities of the lamellar peaks of the α_2 -phase, suggests a packing of the triacylglycerols which has not been considered previously. It is proposed that the metastable α_2 -phase observed at early stages of crystallization has a lamellar structure formed from two types of molecular dimers, one of which corresponds to a typical two-chain packing of TAGs and the other being formed by opposing molecules overlapping by their two-acyl-chain sides. The structural model obtained is phenomenologically similar to smectic A interdigitated phases and synthesizes virtually all the

effects observed in X-ray scattering patterns of the saturated/unsaturated TAGs at the early stages of crystallization where transient metastable phases are present.

It has also been found for the particular case of StOSt that the α_2 -phase can, at some point during the transformation, evolve into a mixed 2L + 3L packing of the molecules. A calculation of X-ray scattering patterns for a structure of randomly packed three-chain and two-chain layers of StOSt, produced by Monte Carlo simulations, reproduced the three diffuse scattering broad peaks observed in the experimental SAXS patterns.

Oleksandr O. Mykhaylyk is grateful for EPSRC funding (grant No. GR/T11852/01).

References

- Chan, K. K., Pershan, P. S., Sorensen, L. B. & Hardouin, F. (1986). *Phys. Rev. A*, **34**, 1420–1433.
- Jong, S. de, van Soest, T. C. & van Schaick, M. A. (1991). *J. Am. Oil Chem. Soc.* **68**, 371–378.
- Kodali, D. R., Atkinson, D., Redgrave, T. G. & Small, D. M. (1987). *J. Lipid Res.* **28**, 403–413.
- Kodali, D. R., Atkinson, D. & Small, D. M. (1990). *J. Lipid Res.* **31**, 1853–1864.
- Lavigne, F., Bourgaux, C. & Ollivon, M. (1993). *J. Phys. IV Colloq.* **3**, 137–140.
- Loisel, C., Keller, G., Lecq, G., Bourgaux, C. & Ollivon, M. (1998). *J. Am. Oil Chem. Soc.* **75**, 425–439.
- Lutton, E. S., Jackson, F. L. & Quimby, O. T. (1948). *J. Am. Oil Chem. Soc.* **70**, 2441–2445.
- Mykhaylyk, O. O. & Hamley, I. W. (2004). *J. Phys. Chem. B*, **108**, 8069–8083.
- Riiner, U. (1970). *Lebensm. Wiss. Technol.* **3**, 101–106.
- Small, D. M. (1986). *The physical chemistry of lipids*. New York: Plenum Press.
- Takeuchi, M., Ueno, S., Floter, E. & Sato, K. (2002). *J. Am. Oil Chem. Soc.* **79**, 627–632.
- Takeuchi, M., Ueno, S., Yano, J., Floter, E. & Sato, K. (2000). *J. Am. Oil Chem. Soc.* **77**, 1243–1249.
- Torbet, J. & Wilkins, M. H. F. (1976). *J. Theor. Biol.* **62**, 447–458.
- Ueno, S., Minato, A., Seto, H., Amemiya, Y. & Sato, K. (1997). *J. Phys. Chem. B*, **101**, 6847–6854.
- Worthington, C. R. (1969). *Biophys. J.* **9**, 222–234.